ChemComm

Improving NanoCluster Beacon performance by blocking the unlabeled NC probes

Journal:	*ChemComm*
Manuscript ID	CC-COM-10-2018-008291.R1
Article Type:	Communication

Journal Name

COMMUNICATION

Improving NanoCluster Beacon performance by blocking the unlabeled NC probes

Received 00th January 20xx,
Accepted 00th January 20xx

DOI: 10.1039/x0xx00000x

www.rsc.org/

Yu-An Chen,†‡[a] Huong T. Vu,‡[a] Yen-Liang Liu,[a] Yuan-I Chen,[a] Trung Duc Nguyen,[a] Yu-An Kuo,[a] Soonwoo Hong,[a] Yin-An Chen,[b] Savannah Carnahan,[c] Jeffrey T. Petty [c] and Hsin-Chih Yeh *[a,d]

While NanoCluster Beacon (NCB) is a versatile molecular probe, it suffers from a low target-specific signal issue due to impurities. Here we show that adding a "blocker" strand to the reaction can effectively block the nonfunctional probes and enhance the target-specific signal by 14 fold at a 0.1 target/probe ratio.

NanoCluster Beacons (NCBs) use a collection of a few atoms of silver as fluorescent reporters and are designed to bind with specific nucleic acid targets, such as pathogenic DNA[1-8]. Once bound with a specific target, a NanoCluster Beacon lights up, emitting fluorescence a hundred to a thousand fold greater than that in the unbound state. The resultant emission can be viewed under ultraviolet (UV) illumination. NanoCluster Beacons come in a rainbow of colors available for multiplexed analysis. Reversible, inexpensive, and easy to use, NanoCluster Beacons are superior molecular probes for detecting targets such as DNA[1], microRNA[9], proteins[10], small molecules[11], cancer cells[12] and enzyme activities[8].

In the original design, an NCB consists of a nanocluster-nucleation strand (hereafter denoted as NC probe) and a G-rich activator strand (denoted as activator probe). These two strands bind in juxtaposition to a DNA target, which enables the G-rich activator sequence to interact with the silver cluster and transform the cluster from a non-emissive species to a highly fluorescent species. Fluorescence thus occurs only when a specific DNA target is present in solution (Figure 1A). As the emission spectra of silver nanoclusters are highly sensitive to their coordination environments (a tunability that is not commonly seen among organic dyes or photoluminescent nanocrystals), NCBs have been turned into multicolor probes for single-nucleotide polymorphism[3] and N^6-methyladenine[7] detection.

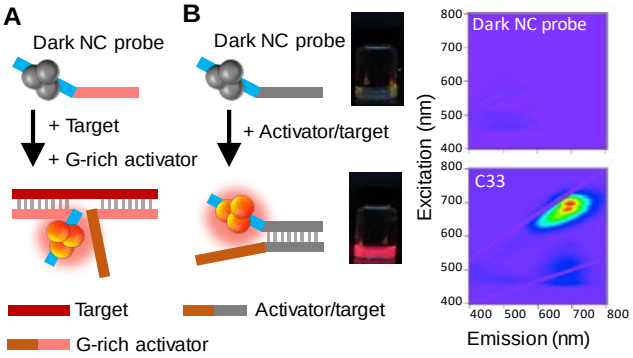

Figure 1. (**A**) Schematics of NanoCluster Beacon (NCB) detection. Consisting of a nanocluster-nucleation (NC) probe and a guanine-rich (G-rich) activator probe, NCB employs DNA-templated, few-atom silver nanocluster as a fluorescent reporter which can significantly light up upon interactions with a G-rich strand nearby (called guanine-proximity-induced fluorescence activation). Upon binding in a juxtaposition to a target, NCB can have its red emission increase by 1500 fold. (**B**) Here we simplify the experiments by eliminating the target strand. Thus, the activator strand plays the roles of both fluorescence activator and target. The pictures and the 2D fluorescence contour plots show NCB fluorescence before and after activation (i.e. with and without binding with the target). C33 is the name of a near-infrared (NIR) emitting NCB under investigation, whose spectral peaks (Ex, Em) locate at (615 nm, 685 nm) and (645 nm, 695 nm).

Whereas NCBs can be conveniently synthesized at room temperature, the synthesis yield, which is the fraction of NC probes that are successfully labeled with an activatable silver cluster, can be as low as 10% (Supplemental Figure S1). The unlabeled NC strands (i.e. nonfunctional NCBs) compete with the labeled strands (i.e. functional NCBs) for binding with targets, thus decreasing the target-specific fluorescence signals (denoted as TSS; see Supplemental Note S1 for TSS definition). Size-exclusion chromatography (SEC) has previously been employed to separate different DNA-templated silver cluster

[a] *Department of Biomedical Engineering, University of Texas at Austin, Austin, Texas, 78712, USA. E-mail: tim.yeh@austin.utexas.edu; Phone: 512-417-7931; Fax: 512-471-0616*
[b] *Department of Chemistry, University of Texas at Austin, Austin, Texas, 78712, USA.*
[c] *Department of Chemistry, Furman University, Greenville, South Carolina, 29613, USA.*
[d] *Department of Biomedical Engineering, University of Texas at Austin, Austin, Texas, 78712, USA.*
† Present address: Laboratory of Systems Pharmacology, Harvard Medical School, Boston, Massachusetts, 02115, USA.
‡ These authors contributed equally.
Electronic Supplementary Information (ESI) available: Explanation of the target specific signal (TSS), experimental methods, DNA sequences, supplemental figures. See DOI: 10.1039/x0xx00000x

species from bare DNA based on their sizes[13] and UV absorbances[14]. However, we found certain types of NCBs (such as the near-infrared (NIR) emitting NCB which we call C33) are difficult to be purified by SEC[6]. While HPLC may be a better way to remove all nonfunctional probes from the solution, such a purification process will add a significant extra cost to the assay.

Here we show a simple blocker strand design that can effectively block the unlabeled probes in the reaction and enhance the target-specific signals. To prove the concept, here we simplify the experiments by eliminating the target strand. The activator strand thus plays the roles of both fluorescence activator and target (Figure 1B). The sequences of the NC-nucleation strand and the activator/target strand for the C33 NIR-emitting NCB can be found in Supplemental Table S1. In our design, the blocker strand also binds with the labeled strand (i.e. functional NCBs), but it can be toehold-displaced by a target strand. In contrast, the target stand cannot displace the blocker strand hybridized with the unlabeled strand. Therefore, by introducing a blocker strand in the solution, we let the target strand preferentially bind with the labeled, functional NCB. At a 0.1 target/probe ratio, the target-specific signal can be enhanced by 14 times when a blocker strand is used. Our strategy can be broadly applied to other NCB designs to enhance the target-specific signals.

To grow dark but activatable silver nanoclusters in the NC probes, we first incubate 15 μM DNA with 180 μM silver nitrate in a 20 mM pH 6.6 sodium phosphate buffer. A reducing agent, sodium borohydride, is then added to the solution, reaching a final concentration of 90 μM ([DNA]:[Ag^+]:[$NaBH_4$]=1:12:6). The sample is then set aside overnight in the dark at room temperature before use. As we demonstrated previously, the silver cluster nucleation reaction created a mixture of "unlabeled and labeled" NC probes (i.e. nonfunctional and functional NCBs, denoted as **1** and **2** in Figure 2A). The successfully labeled NC probes (with dark but activatable silver clusters encapsulated) exhibited a 10-30 second longer retention time in SEC as compared to the unlabeled NC probes, indicating a 6-18 % decrease in size after silver cluster encapsulation[6]. By comparing the autocorrelation curve of activated NC probes to that of an HPLC-purified ATTO633-labeled DNA strand in fluorescence correlation spectroscopy (FCS), we found synthesis yield of functional C33 NC probes to be ~10% (Supplemental Figure S1). With a 10% yield, we expect 10% of targets to bind with labeled NC probes, leading to 10% of target-specific signal (TSS, see Supplemental Note 1 and Figure S2A for more discussion). Nevertheless, we achieve 10% of TSS only when the target/probe ratio is at 1:1. At a lower target/probe ratio, such as 0.5, the observed TSS is substantially less than 10% (Supplemental Figure S2B). This indicates that when probes are abundant, targets may preferentially bind with the unlabeled NC probes rather than the labeled ones.

To recover TSS, we design a blocker strand (termed compC33_+15, denoted as **3** in Figure 2A) that preferentially binds with unlabeled NC probes. This compC33_+15 blocker strand is designed to have a portion that is complementary to the NC-nucleation region on the NC probe, plus additional 15 nucleotides that are complementary to the hybridization

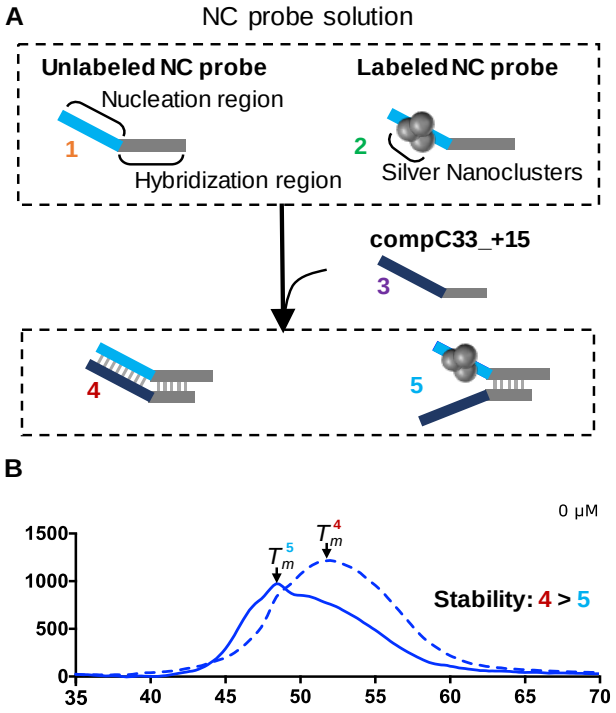

Figure 2. (**A**) Schematics showing different single-stranded and double-stranded species in the sample. Here the unlabeled and the labeled NC probes are denoted as species **1** and **2**. They coexist in the NC probe solution because the silver nucleation process on DNA typically has yield far less than 100%. After adding a blocker strand (named compC33_+15, species **3**) to the sample, two duplexes, duplexes **4** and **5**, are formed. The blocker **3** is designed to preferentially bind with the unlabeled NC probe **1**, forming duplex **4**. (**B**) High-resolution melting (HRM) analysis of the NC probe mixtures demonstrates that duplex **4** is more thermodynamically stable than duplex **5**. Note that the C33 NC probe itself is a mixture of species **1** and **2**. After binding with the blocker **3**, the resulting first-derivative melting curve exhibits multiple peaks (solid line). When 5 μM of additional duplex **4** is added to the sample, the melting curve shifts to the right (dashed line). Thus we believe duplex **4** has the melting temperature (T_m^4) around 52°C while duplex **5** has the melting temperature (T_m^5) around 48°C.

sequence (Figure 2A and Supplemental Table S1). From high-resolution melting (HRM) analysis[7, 15] (Figure 2B), we noticed a multiple-peak feature in the first-derivative melting curves, suggesting the presence of both the blocker-unlabeled NC strand duplex and the blocker-labeled NC strand duplex (denoted as **4** and **5**, respectively) in both samples. When there are more blocker-unlabeled NC strand duplexes (duplex **4**) in the solution, the melting temperature increases (Figure 2B), proving that the blocker-unlabeled NC strand duplex **4** is indeed more thermodynamically stable than its labeled counterpart duplex **5**.

Since the blocker strands preferentially bind with the unlabeled NC probes, biotinylated blocker strands and streptavidin-coated magnetic beads can be used to selectively remove the unlabeled NC probes from the solution (Supplemental Figure S3). Indeed, after bead purification, the amount of unlabeled NC probes is found greatly reduced in the size-exclusion chromatograms. As expected, after removal of unlabeled NC probes, TSS is enhanced by 2.5-fold at a 0.5 target/probe ratio. Whereas removal of unlabeled NC probes is a straightforward method to recover TSS, this additional

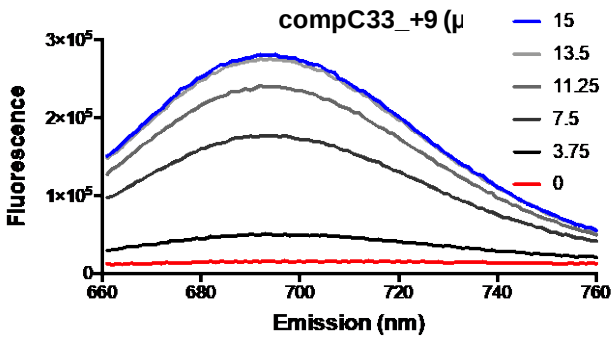

Figure 3. Recovery of target-specific signal (TSS) by adding a blocker strand (compC33_+9) to the reaction. The target/probe ratio was fixed at 0.1 in this experiment (1.5 μM for the activator/target strand NC strand and 15 μM for the NC strand). The concentration of the blocker strand (compC33_+9) increased from 0 μM to 15 μM. The emission spectra were measured under 645 nm excitation.

purification step adds to the cost of the assay. We prefer rescuing TSS without using bead purification.

Here we prove that we can restore the 10% TSS by simply adding a blocker strand to the detection reaction. For a sample at a 0.1 target/probe ratio, without using any blocker strand, the TSS is only slightly higher than the background fluorescence (here the background means the fluorescence from the sample that has the NC probes only, without any activator/target strands). As we start adding blocker strand to the sample, the fluorescence is recovered (Figure 3). We find that the fluorescence recovery is maximized by 14 times when the blocker concentration is equal to the NC probe concentration. Similar TSS recovery results are also seen in a sample at 0.5 target/probe ratio (Supplemental Figure S4).

To further enhance the TSS recovery, it is necessary to fine-tune the affinity between the blocker strand and the target. On one hand, the additional base-pairing region (the +n part) has to be long enough to ensure stable binding between the blocker and the unlabeled probe, thus providing a sufficient blocking effect. On the other hand, the additional base-pairing region cannot be too long so that the blocker can be easily toehold displaced from the labeled NC strand by a target strand. Nine blocker strands with different lengths of the additional base-pairing region (compC33_+6 to compC33_+30; see DNA list in Supplemental Table S1) were synthesized and tested. In this optimization experiment, the target/probe/blocker concentrations were kept at 2.5:5:5 μM (0.5:1:1). When the TSS of the first 5:5:0 μM sample (1.8×10^6 AU) was set to be 10% (considering the synthesis yield; the tall black bar in Figure 4A), the resulting TSS of the second 2.5:2.5:0 μM sample was about 11% (short black bar). The TSS of the third 2.5:5:0 μM was 7.6% (red bar), which was lower than 11% because targets tended to bind with unlabeled NC probes.

By using blockers with different lengths, we not only fully restored the expected 10% TSS but also achieved an even higher TSS (16%) when compC33_+15 blocker was used. This higher-than-expected TSS indicated that the blocker assisted the targets to preferentially bind with the labeled NC probes. To investigate how the blocker strand blocks the unlabeled NC probe, we have conducted SEC on the mixtures of NC probes and blocker strands, without the activator/target strands

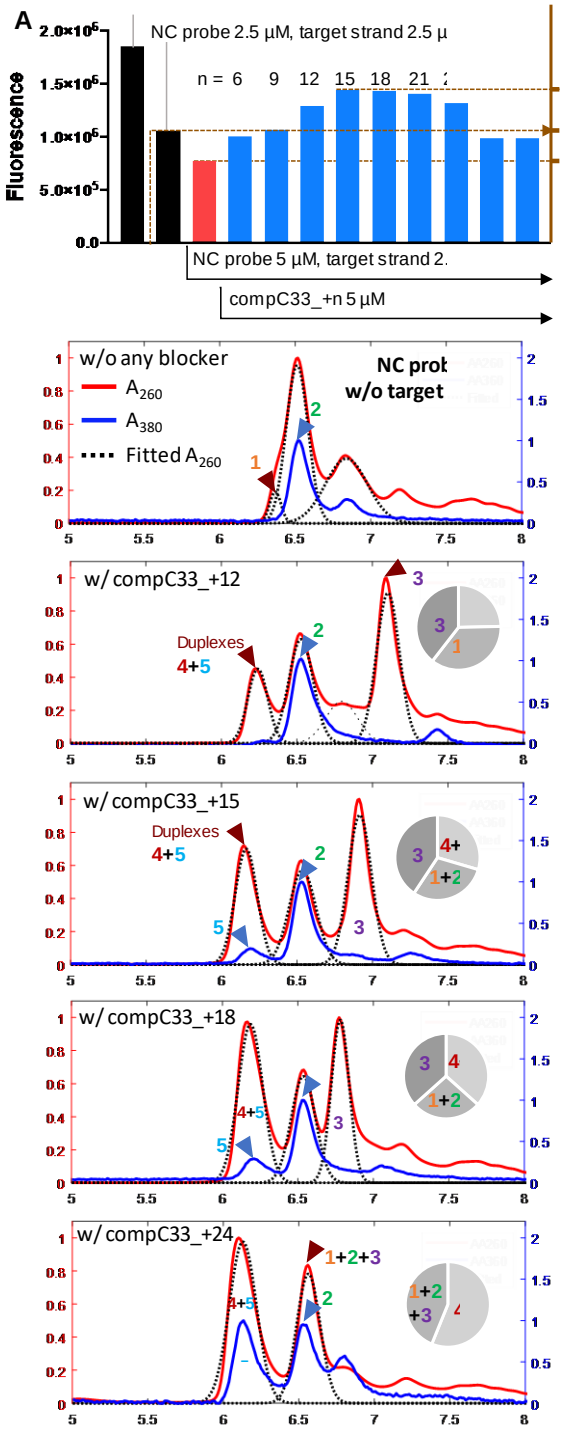

Figure 4. (**A**) The effect of fluorescence recovery based on various lengths of blockers (compC33_+n). The emission intensities are integrated from 660 nm to 760 nm, under 645 nm excitation. (**B**) Size-exclusion chromatograms of five samples. The top plot is the sample with C33 NC probe only (which is a mixture of species **1** and **2**), without any blocker stand or activator/target strand. The rest four samples are mixing the C33 NC probe with various lengths of blocker strands (compC33_+12 to compC33_+24). Absorption peaks at 260 nm (red) and 380 nm (blue) represent the DNA strands and the silver nanocluster, respectively. A multi-Gaussian fitting (dash lines) is used to discerned the different species in the sample, which are indicated in the chromatograms based on their numbers assigned in Figure 2. The pie charts represent the relative populations of various species in the samples. Other smaller peaks correspond to impurities or partially folded strands and are not considered. The trend in fluorescence characterization in (A) matches well with the SEC results. The optimal blocker design is around compC33_+15.

(Figure 4B). Absorbance at 260 nm (A_{260}) and 380 nm (A_{380}) were used to indicate the DNA strands and the silver nanoclusters, respectively. In the top chromatogram of Figure 4B, the "shoulder" of the A_{260} curve at 6.3 min retention time presents a species with a strong 260 nm absorption but no 380 nm absorption, which we believe to be the unlabeled NC probe (species **1**). The A_{260} and A_{380} curves both have a peak at 6.5 min retention time, which should be corresponding to the silver cluster-labeled NC probe (species **2**). Figure S3A was showing a similar result, but with well-separated peaks.

In the chromatograms 2-5 of Figure 4B, different lengths of blocker strands were added to the samples. As the blocker strands were shorter than the labeled NC probe, the free blocker strands (species **3**) had retention times longer than that of the labeled NC probe (from 6.6 to 7.2 min). When the long blocker compC33_+24 was used, the blocker's A_{260} peak eventually merged with that of the labeled NC probe. This was because the physical sizes of the labeled NC and the compC33_+24 blocker were about the same. Note that the A_{260} peaks around 6.2 min retention time were corresponding to the duplex species **4** and **5** (as these duplexes had sizes larger than that of the labeled NC probe). Due to their similar sizes, species **4** and **5** were not differentiable in the chromatograms.

The results showed that as the length of blockers was increased from +6 to +15, higher target-specific signals (TSS) were observed. The TSS reached a maximum (16%) when the compC33_+15 blocker was used. As shown in Figure 4B, when the blocker compC33_+12 was used, the duplex species **4** formation was relatively low, suggesting a relatively lower blocking effect. As the length of the blocker kept increasing, more duplex species **4** were formed (better blocking). However, at the same time more duplex species **5** were also formed (shown as the blue A_{380} peak at 6.2 min retention time). In other words, the longer blockers (+18 to +30) block "the labeled NC probes that they are not supposed to block". We thus conclude the medium-length blocker, compC33_+15, is the optimal blocker design for C33 NCB.

In this study, we characterize the synthesis yield of the NIR-emitting C33 NanoCluster Beacon and point out the low target-specific signal issue in current NCB detection. While there is no doubt that the TSS can be at 100% if there is no nonfunctional NCB in solution (i.e. every target is guaranteed to bind with a functional probe), at this moment it is difficult and expensive to completely remove all unlabeled NC probes (i.e. nonfunctional NCB) from solution. Even with 10% synthetic yield, researchers can still use NCB for many in-vitro, surface-based staining applications[8]. But we do not always get the 10% target-specific signal as targets may preferentially bind with the unlabeled probes. To recover the 10% target-specific signal or further enhance that, here we demonstrate a simple blocker design that effectively block the unlabeled probes in the reaction. While enhancing the synthesis yield to 100% or completely removing all unlabeled probes is the ultimate solution, our method provides a cost-effective method to rescue the TSS in NCB detection. Our results can be generally applied to many NCB detection applications in molecular and cellular biology[3-5, 7, 8].

This research is financially supported by Robert A. Welch Foundation (F-1833 to H.-C.Y.) and National Science Foundation (Grant 1611451). Jeff Petty also thanks the National Institutes of Health (1R15GM102818) and the National Science Foundation EPSCoR Program under NSF Award # OIA-1655740.

Conflicts of interest

There are no conflicts to declare.

References

1 H.-C. Yeh, J. Sharma, J. J. Han, J. S. Martinez and J. H. Werner, *Nano letters*, 2010, **10**, 3106-3110.
2 H.-C. Yeh, J. Sharma, J. J. Han, J. S. Martinez and J. H. Werner, *IEEE Nanotechnology Magazine*, 2011, **5**, 28-33.
3 H.-C. Yeh, J. Sharma, M. Shih Ie, D. M. Vu, J. S. Martinez and J. H. Werner, *J Am Chem Soc*, 2012, **134**, 11550-11558.
4 J. M. Obliosca, C. Liu, R. A. Batson, M. C. Babin, J. H. Werner and H.-C. Yeh, *Biosensors*, 2013, **3**, 185-200.
5 J. M. Obliosca, C. Liu and H.-C. Yeh, *Nanoscale*, 2013, **5**, 8443-8461.
6 J. M. Obliosca, M. C. Babin, C. Liu, Y.-L. Liu, Y.-A. Chen, R. A. Batson, M. Ganguly, J. T. Petty and H.-C. Yeh, *Acs Nano*, 2014, **8**, 10150-10160.
7 Y.-A. Chen, J. M. Obliosca, Y.-L. Liu, C. Liu, M. L. Gwozdz and H.-C. Yeh, *J Am Chem Soc*, 2015, **137**, 10476-10479.
8 S. Juul, J. M. Obliosca, C. Liu, Y.-L. Liu, Y.-A. Chen, D. M. Imphean, B. R. Knudsen, Y.-P. Ho, K. W. Leong and H.-C. Yeh, *Nanoscale*, 2015, **7**, 8332-8337.
9 J. Zhang, C. Li, X. Zhi, G. A. Ramón, Y. Liu, C. Zhang, F. Pan and D. Cui, *Anal Chem*, 2015.
10 J. J. Li, X. Q. Zhong, H. Q. Zhang, X. C. Le and J. J. Zhu, *Anal Chem*, 2012, **84**, 5170-5174.
11 M. Zhang, S. M. Guo, Y. R. Li, P. Zuo and B. C. Ye, *Chemical Communication*, 2012, **48**, 5488-5490.
12 J. Yin, X. He, K. Wang, F. Xu, J. Shangguan, D. He and H. Shi, *Anal Chem*, 2013, **85**, 12011-12019.
13 J. T. Petty, B. Giri, I. C. Miller, D. A. Nicholson, O. O. Sergev, T. M. Banks and S. P. Story, *Anal Chem*, 2013.
14 P. R. O'Neill, L. R. Velazquez, D. G. Dunn, E. G. Gwinn and D. K. Fygenson, *J Phys Chem C*, 2009, **113**, 4229-4233.
15 J. M. Obliosca, S. Y. Cheng, Y.-A. Chen, M. F. Llanos, Y.-L. Liu, D. M. Imphean, D. Bell, J. T. Petty, P. Ren and H.-C. Yeh, *J Am Chem Soc*, 2017.